26th ABCM International Congress of Mechanical Engineering
November 22-26, 2021. Florianópolis, SC, Brazil

COB-2021-1730
USE OF LATERAL DYNAMICS AND THE LEVENBERG-MARQUARDT METHOD TO ESTIMATE PARAMETERS OF A PICKUP TRUCK

Adrián Eduardo Simioni
Victor Santoro Santiago
Bruna Rafaella Loiola
Ricardo Teixeira da Costa Neto
Camila Leão Pereira
Military Institute of Engineering – Praça Gen. Tibúrcio, 80 – Urca - Rio de Janeiro, RJ - Brasil - 22290-270
aesimioni@gmail.com, santoro@ime.eb.br, bruna.loiola@ime.eb.br, ricardo@ime.eb.br, camilaleaop@gmail.com

Abstract. *Numerical analysis and computational solutions are widespread among automotive engineering projects, mainly in the early stages where uncertainties and lack of data play an important role and become some of the main problems to be solved by designers. In cases where a utility vehicle is adapted to transport a special module, care must be taken with the variability of its parameters. This type of modification usually changes the vehicle's center of gravity from its primary position, which makes the maneuvers difficult to be performed at higher speeds, increasing the tendency to rollover. Thus, a methodology is proposed to evaluate the behavior of the lateral dynamics of a utility vehicle weighing up to 3,500 kgf which has its original bucket replaced by another with a military application, finding new parameters that allow it to maintain its performance in curves as close as possible of the original. Therefore, it was chosen to estimate the spring stiffness and parameters of the suspension dampers for this new configuration. In this work, a model of 4 degrees of freedom is applied considering the lateral and longitudinal dynamics of a vehicle in a double lane change test and considering the model proposed by Dugoff to represent the behavior of the tires. The numerical solution was obtained in the MATLAB / Simulink® software using the Power Flow method. Numerical verification was performed by comparing the dynamic response behavior of the proposed model with results from the Carsim® software, which is a commercial package used in vehicle development. The inverse analysis was performed by the Levenberg-Marquardt method considering the measurements of the roll angle during a double lane change maneuver. The estimated suspension constants allow necessary changes to be made to the vehicle's characteristics, adapting requirements and improving its dynamic behavior, reducing time, accident risks, costs and other resources that can be used in later stages of the project.*

Keywords: *lateral dynamics, nonlinear tire model, inverse problems, Levenberg-Marquardt method.*

1. INTRODUCTION

The use of pickup vehicles has recently increased over utility vehicles due to the possibility of adding different load modules as pickup box. However, such change implies on modification of the original configuration, since the relations established in the early stages of suspension, load transfer and weights development must be adapted to the updated requirements. In this regard, this work intends to estimate the suspension constants of a modified vehicle. In order to perform this study, a well-established mathematical model is applied to simulate the spatial dynamics of the proposed system considering tire deformation model in rigid soil. The inverse analysis is then applied through Levenberg-Marquardt method to estimate and correctly adjust the constants of the suspension using measurements of the roll angle produced in a curve maneuver. This technique was already applied to estimate the tires' cornering stiffness of a 6x6 vehicle through an inverse problem formulation using the yaw rate field measurement during a double lane change test maneuver and the mathematical model of the vehicle's lateral dynamics (Leão Pereira, C., 2020; Leão Pereira, C., Costa Neto, R.T., and Loiola, B.R., 2021). Two vehicle models (loaded and unloaded vehicles) will be developed, addressing the power flow methodology (Costa Neto, 2001) to model the longitudinal, vertical and lateral dynamics subsystems, as well as their interrelationships. For the comparison of the models, the simulation of the double lane change test (ISO 3888) at constant speed will be used, in order to generate the rolling of the sprung mass and a controlled lateral load transfer, which allows the suspension to be activated and the modeling of the non-linear tire model due to the development of combined longitudinal and lateral forces in the area of contact with the ground (Dugoff, 1970).

2. VEHICLE DYNAMICS

The dynamic behavior of a vehicle could be studied through its longitudinal, lateral and vertical dynamics. Initially, the reference system is defined in the mass center of the chassis, adopting the ISO 4130 coordinate system, as shown in

Figure 1, (Gillespie, 1992). This model presents a dynamic behavior that originally confers 6 degrees of freedom (DOF) with three translation movements (displacements in the x, y and z axes) and three rotation movements in the local reference (pitch (θ) - yaw (ψ) - roll (φ)).

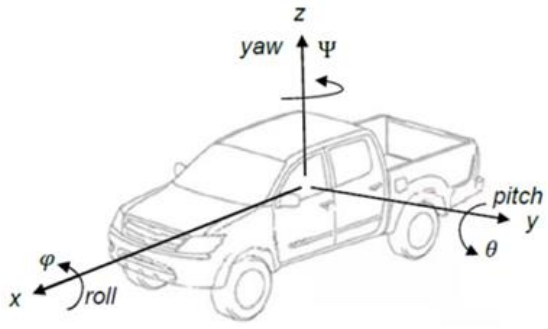

Figure 1. Vehicle coordinate system (ISO 4130).

For the vehicle modelled in this work, a 4 DOF model is considered based on the assumptions (Will and AK, 1997) that the vehicle is composed of three masses: one suspended mass and two unsprung masses, the effects of power train are taking into account; the tires of the vehicle are considered in permanent contact with the ground during the test; tire rolling resistance, drag and aerodynamic forces are negligible; lateral and longitudinal forces are functions of the normal forces and of the slip angles of the tires; tires forces is considered in the *x*-*y* plane of the vehicle, in which the bounce movement is not considered (displacement in *z*); the chassis inclination angles are considered small; and the test is performed at a constant speed, so longitudinal weight transfer and pitch movement is not considered. In this sense, the 4 DOF for the non-linear model of the vehicle are represented by the displacement in the *x* axis, the displacement in the *y* axis, the rotation around the *z* axis - yaw movement (ψ) - and the rotation around the x axis – roll motion (φ).

2.1 Equations of motion

The chosen model, proposed by Will and AK (1997) and Lima Spinola (2003), describes the rotation and translation movement of the suspended mass using fixed axes in the vehicle body where Newton-Euler equations of motion for the non-linear 4 DOF model can be set in the form of state space to represent the dynamic behaviour according to Eq. (1).

$$\begin{bmatrix} m_t & 0 & 0 & 0 \\ 0 & m_t & 0 & m_s h_s \\ 0 & 0 & I_z & 0 \\ 0 & m_s h_s & 0 & I_{roll} \end{bmatrix} \begin{bmatrix} \ddot{x} \\ \ddot{y} \\ \ddot{\psi} \\ \ddot{\varphi} \end{bmatrix} = \begin{bmatrix} m_t \dot{y}\dot{\psi} \\ -m_t \dot{x}\dot{\psi} \\ 0 \\ -\beta_{roll}\dot{\varphi} - K_{roll}\varphi + m_s g h_s \varphi - m_s h_s \dot{x}\dot{\psi} \end{bmatrix} + \begin{bmatrix} F_x \\ F_y \\ M_z \\ 0 \end{bmatrix} \quad (1)$$

where F_x, F_y, M_z, m_t, m_s, I_z, I_{roll}, h_s, β_{roll}, K_{roll} and g are the longitudinal force, lateral force, yawing moment, total mass, sprung mass, moment of inertia (z-axis), moment of inertia (x-axis), height of the roll center, rolling dumping, rolling stiffness and gravity acceleration, respectively, and $\ddot{x}$, $\ddot{y}$, $\ddot{\psi}$, $\ddot{\varphi}$ and $\dot{x}$, $\dot{y}$, $\dot{\psi}$, $\dot{\varphi}$ are the acceleration and velocity of x and y displacements, yaw (ψ) and roll (φ) angles.

2.2 Slip angle

The slip angles (α) for each tire: front left (*FL*), front right (*FR*), rear left (*RL*) and rear right (*RR*) are represented in Eqs. (2) to (5) as function of the front (δ_f) and rear steering angle (δ_r), longitudinal speeds $\dot{x}$, lateral speeds $\dot{y}$, yaw angle speeds ($\dot{\psi}$), front (t_f) and rear track (t_r), and the position of the tires in relation to the mass center (constants *a* and *b*).

$$\alpha_{FL} = \delta_f - atan\left(\frac{\dot{y} + a\dot{\psi}}{\dot{x} - \frac{t_f}{2}\dot{\psi}}\right) \quad (2)$$

$$\alpha_{FR} = \delta_f - atan\left(\frac{\dot{y} + a\dot{\psi}}{\dot{x} + \frac{t_f}{2}\dot{\psi}}\right) \quad (3)$$

$$\alpha_{RL} = \delta_r + atan\left(\frac{\dot{y} - b\dot{\psi}}{\dot{x} - \frac{t_r}{2}\dot{\psi}}\right) \tag{4}$$

$$\alpha_{RR} = \delta_r + atan\left(\frac{\dot{y} - b\dot{\psi}}{\dot{x} + \frac{t_r}{2}\dot{\psi}}\right) \tag{5}$$

2.3 Normal forces

Normal forces are generated by the load transfer, identified as: the load due to the vehicle roll, Eq. (6) and Eq. (7); the load due to the height of the roll center, Eq. (8) and Eq. (9); and the load due to the unsprung masses (m_u), Eq. (10) and Eq. (11). In all equations, the subscript f and r are for front and rear suspensions, respectively.

$$F_{rf} = \frac{K_f h_s m_s a_y}{k_{roll} t_f} \tag{6}$$

$$F_{rr} = \frac{K_r h_s m_s a_y}{k_{roll} t_r} \tag{7}$$

$$F_{hf} = \frac{m_s b h_f a_y}{t_f (a+b)} \tag{8}$$

$$F_{hr} = \frac{m_s a h_r a_y}{t_r (a+b)} \tag{9}$$

$$F_{uf} = m_{uf} a_y \frac{h_f}{t_f} \tag{10}$$

$$F_{ur} = m_{ur} a_y \frac{h_f}{t_f} \tag{11}$$

There is a load due to the longitudinal transfer of weight by braking, subscript b, according to Eq. (12) and Eq. (13), and also another for the static load acting on the tires, subscript s, according to Eq. (14) and (15).

$$F_{bf} = (\, m_{uf}\, h_f + m_s\, h_{cg} + \, m_{ur} h_r\,) \frac{a_x}{a+b} \tag{12}$$

$$F_{br} = -\big(\, m_{uf}\, h_f + m_s\, h_{cg+}\, m_{ur} h_r\,\big) \frac{a_x}{a+b} \tag{13}$$

$$F_{Nsf} = \frac{b\, m_t\, \mathrm{g}}{a+b} \tag{14}$$

$$F_{Nsr} = \frac{a\, m_t\, \mathrm{g}}{a+b} \tag{15}$$

Considering the terms mentioned before, the vertical forces of each tire are presented, according to Eq. (16) to (19):

$$F_{zFL} = -F_{rf} - F_{hf} - F_{uf} - \frac{1}{2}F_{bf} + \frac{1}{2}F_{Nsf} \tag{16}$$

$$F_{zFR} = F_{rf} + F_{hf} + F_{uf} - \frac{1}{2}F_{bf} + \frac{1}{2}F_{Nsf} \tag{17}$$

$$F_{zRL} = -F_{rr} - F_{hr} - F_{ur} - \frac{1}{2}F_{br} + \frac{1}{2}F_{Nsr} \tag{18}$$

$$F_{zRR} = F_{rr} + F_{hr} + F_{ur} - \frac{1}{2}F_{br} + \frac{1}{2}F_{Nsr} \tag{19}$$

2.4 Tire lateral forces

The generation of high lateral accelerations and combined forces in the tires when driving in curves lead to the use of non-linear tire models (Smith, 2007). Dugoff (1970) developed a non-linear tire model based on the adhesion ellipse concept, which depends on slip angles, lateral stiffness when cornering, and on the longitudinal slip of the tire, Eq. (20),

$$L_i = \frac{C_\alpha \, tan\, \alpha_i}{1 - i_s} \, f(s) \tag{20}$$

where $f(s)$ is the characteristic adhesion ratio of the tire, described by Eq. (21) and Eq. (22).

$$f(s) = \begin{cases} s(2-s) & if \;\; s \leq 1 \\ 1 & if \;\; s > 1 \end{cases} \tag{21}$$

$$s = \frac{\mu F_{Ni}\left(1 - \varepsilon_r \, U \, \sqrt{i_s^2 + tan^2 \alpha_i}\right)}{2\sqrt{C_x^2 \, i_s^2 + \, C_\alpha^2 \, tan^2 \alpha_i}} \, (1 - i_s) \tag{22}$$

where s is the adhesion of the tire, μ is the adhesion coefficient to the track, F_{Ni} is the normal force of the i-th tire, ϵ_r is the factor of track adhesion reduction, U is longitudinal speed, i_s is the longitudinal slip, C_s is longitudinal stiffness, C_α is lateral stiffness, and α_i is the slip angle of the i-th tire. Figure 2 shows the interrelations between normal forces, slip angle and lateral force, to which each tire is subjected, according to the points 2.3, 2.4, and 2.5 already established.

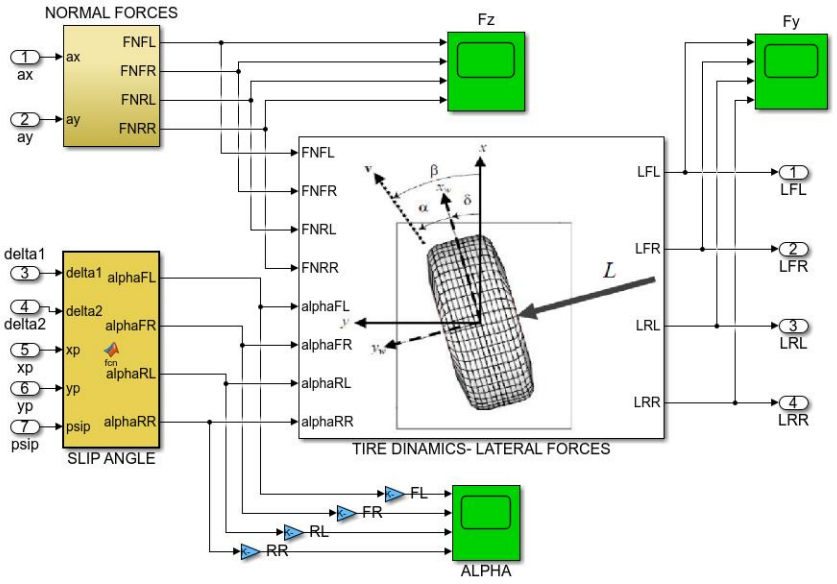

Figure 2. Tire dynamics (photo by Jazar (2008), adapted by the author).

2.5 Sum of forces and moments

After defined the relations of forces to the tires, it is possible to write the forces and the resulting moments. The forces, represented by Eq. (23) to (24), will be dependent on the input variables: front steering angle (δ_f); rear steering angle (δ_r); brake pedal angle (δ_b); lateral forces (L); and tire stiffness coefficients (C).

$$F_x = -(C_{FL} + C_{FR})\delta_b \cos \delta_f - (C_{RL} + C_{RR})\delta_b \cos \delta_r - (L_{FL} + L_{FR}) \sin \, \delta_f - (L_{RL} + L_{RR}) \sin \, \delta_r \tag{23}$$

$$F_y = -(C_{FL} + C_{FR})\delta_b \, sin \, \delta_f - (C_{RL} + C_{RR})\delta_b \, sin \, \delta_r + (L_{FL} + L_{FR}) \, cos \, \delta_f + (L_{RL} + L_{RR}) cos \, \delta_r \tag{24}$$

The yaw moment is calculated for each tire according to Eq. (25) to (26), the summation is given at Eq. (29).

$$M_{FL} = -\delta_b\, C_{FL}\, a\, sin\, \delta_f\, -\, \delta_b\, C_{FL}\, \frac{t_f}{2} \cos \delta_f + \, a\, L_{FL} \cos \delta_f\, - \frac{t_f}{2} L_{FL}\, sin\, \delta_f \tag{25}$$

$$M_{FR} = -\delta_b\, C_{FR}\, \, a\, sin\, \delta_f - \delta_b\, C_{FR}\, \, \frac{t_f}{2}\, cos\, \delta_f + \, a\, L_{FR}\, \cos \delta_f\, -\, \, \frac{t_f}{2} L_{FR}\, \, sin\, \delta_f \tag{26}$$

$$M_{RL} = \, \delta_b\, C_{RL}\, \, b\, sin\, \delta_r - \delta_b\, C_{RL}\, \, \frac{t_f}{2}\, cos\, \delta_r - \, b\, L_{RL}\, \, cos\, \delta_r\, -\, \, \frac{t_f}{2} L_{RL}\, \, sin\, \delta_r \tag{27}$$

$$M_{RR} = \delta_b\, C_{RR}\, \, b\, sin\, \delta_r - \delta_b\, C_{RR}\, \, \frac{t_f}{2}\, cos\, \delta_r\, \, - \, b\, L_{RR}\, \, cos\, \delta_r\, -\, \, \frac{t_f}{2} L_{RR}\, \, sin\, \delta_r \tag{28}$$

$$M = \, \, M_{FL} + \, \, M_{FR} + M_{RL} + M_{RR} \tag{29}$$

2.6 Model representation in the state-space format

Taking into account the components of F_x, F_y and M_z of the nonlinear model, it is possible to perform some manipulations to represent them in the state-space format, Eq. (30).

$$M^{-1} = \begin{bmatrix} \frac{1}{m_t} & 0 & 0 & 0 \\ 0 & \frac{I_{roll}}{m_t\, I_{roll} - (m_s h_s)^2} & 0 & \frac{-m_s h_s}{m_t\, I_{roll} - (m_s h_s)^2} \\ 0 & 0 & \frac{1}{I_z} & 0 \\ 0 & \frac{-m_s h_s}{m_t\, I_{roll} - (m_s h_s)^2} & 0 & \frac{m_t}{m_t\, I_{roll} - (m_s h_s)^2} \end{bmatrix} \tag{30}$$

In this particular case, Eq. (31) represents the non-linear model of four degrees of freedom in the local frame, located in the vehicle itself.

$$\begin{bmatrix} \ddot{x} \\ \ddot{y} \\ \ddot{\psi} \\ \ddot{\varphi} \end{bmatrix} = \begin{bmatrix} \dot{y}\dot{\psi} \\ \frac{m_s h_s \beta_{roll} \dot{\varphi} + m_s h_s (K_{roll} - m_s h_s\, \mathrm{g})\varphi}{m_t\, I_{roll} - (m_s h_s)^2} \\ 0 \\ \frac{m_t\, (m_s h_s\, \mathrm{g}\, \varphi - \beta_{roll} \dot{\varphi} - K_{roll})}{m_t\, I_{roll} - (m_s h_s)^2} \end{bmatrix} + \begin{bmatrix} \frac{F_x}{m_t} \\ \frac{F_y\, I_{roll}}{m_t\, I_{roll} - (m_s h_s)^2} \\ \frac{M_z}{I_z} \\ \frac{-F_y\, m_s h_s}{m_t\, I_{roll} - (m_s h_s)^2} \end{bmatrix} \tag{31}$$

Therefore, to observe the displacement in the global framework, it is necessary to consider the longitudinal and lateral velocities on the global framework, showed in Eq. (32) and Eq. (33).

$$\dot{X} = \dot{x}\, cos\, \psi - \, \, \dot{y}\, sin\, \psi \tag{32}$$

$$\dot{Y} = \dot{x}\, sin\, \psi + \, \, \dot{y}\, cos\, \psi \tag{33}$$

In order to represent the longitudinal, lateral and angular displacements and velocities, it is necessary to expand the state vector, renaming it according to Eq. (34).

$$\begin{bmatrix} x_1 \\ x_2 \\ x_3 \\ x_4 \\ x_5 \\ x_6 \\ x_7 \\ x_8 \\ x_9 \\ x_{10} \end{bmatrix} = \begin{bmatrix} x \\ \dot{x} \\ y \\ \dot{y} \\ \psi \\ \dot{\psi} \\ \varphi \\ \dot{\varphi} \\ X \\ Y \end{bmatrix} \quad \text{and} \quad \begin{bmatrix} u_1 \\ u_2 \\ u_3 \end{bmatrix} = \begin{bmatrix} \delta_f \\ \delta_r \\ \delta_b \end{bmatrix} \tag{34}$$

In this case, considering Eq. (23), Eq. (24), Eq. (29), Eq. (31) and Eq. (34), we obtain the equations of the non-linear model of four degrees of freedom that describes the lateral dynamics of the vehicle (Eq. 35). It should be noted that the steering angles of the front wheels δ_f are the main input of the model and that the steering angles of the rear wheels δ_r and the brake pedal δ_b are included within the power block and moments, although in this particular case they are not considered.

$$\begin{bmatrix} \dot{x}_1 \\ \dot{x}_2 \\ \dot{x}_3 \\ \dot{x}_4 \\ \dot{x}_5 \\ \dot{x}_6 \\ \dot{x}_7 \\ \dot{x}_8 \\ \dot{x}_9 \\ \dot{x}_{10} \end{bmatrix} = \begin{bmatrix} x_2 \\ x_4 x_6 + \dfrac{F_x}{m_t} \\ x_4 \\ -x_2 x_6 + \dfrac{[m_s h_s K_{roll} - (m_s h_s)^2 \mathrm{g}] x_7 + m_s h_s \beta_{roll} x_8 + I_{roll} F_y}{m_t\, I_{roll} - (m_s h_s)^2} \\ x_6 \\ \dfrac{M}{I_z} \\ x_8 \\ \dfrac{m_t[(m_s h_s\, \mathrm{g} - K_{roll}) x_7 - \beta_{roll} x_8] - m_s h_s F_y}{m_t\, I_{roll} - (m_s h_s)^2} \\ x_2\, cos\, x_5 - x_4\, sin\, x_5 \\ x_2\, sin\, x_5 - x_4\, cos\, x_5 \end{bmatrix} \tag{35}$$

Finally, Figure 3 shows the architecture developed in a MATLAB / Simulink® block diagram of the dynamic 4 DOF model, executing the ISO 3888 double lane change test, where all the equations previously presented were considered.

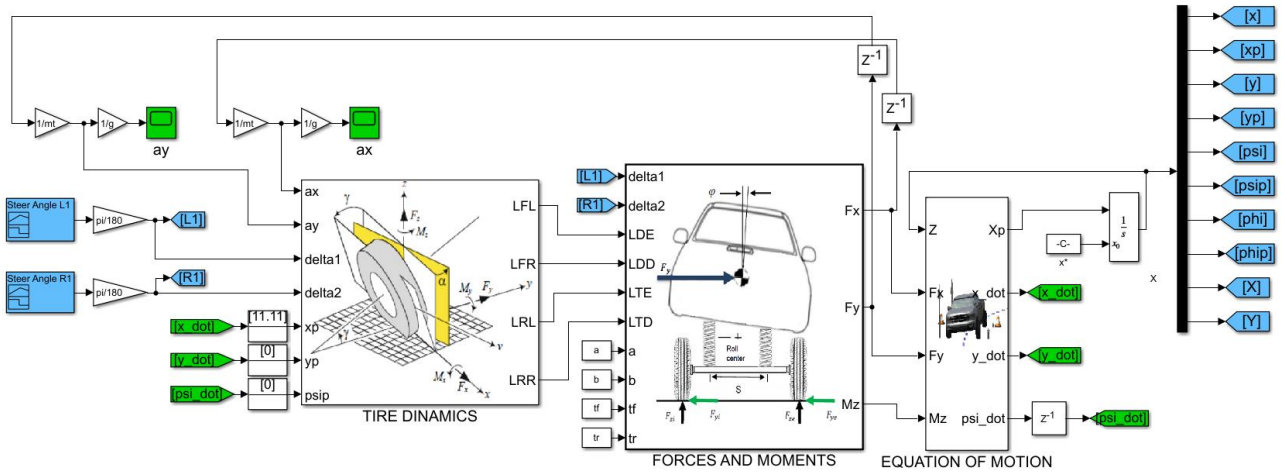

Figure 3. Four degrees of freedom model. (Photo by Jazar (2008), adapted by the author)

3. INVERSE PROBLEMS

3.1 Método de Levenberg Marquardt

Some mathematical and computational models are often used in vehicle dynamics studies, helping to optimize and adjust parameters that are usually obtained by experimental methods. This approach avoids risks and resources waste. Therefore, considering the inaccuracy from experimental data or the lack of them, the development of inverse problems for parameters estimation through model-dependent variables is formulated. In this work, the LM method is used, which makes the estimation of parameters by means of an iterative procedure that considers the hypothesis of additive errors, without bias and uncorrelated measures (Cortez, 2004). Thus, this solution via inverse problems for the estimation of *n* unknown parameters *Pj*, being *j = 1,2,3 ... n*, is based on minimizing the function of maximum likelihood objective $S(\boldsymbol{P})$ given in Eq. (36).

$$S(\mathbf{P}) = \left[\mathbf{Y} - \hat{\mathbf{Y}}(\mathbf{P})\right]^T \mathbf{W^{-1}} \left[\mathbf{Y} - \hat{\mathbf{Y}}(\mathbf{P})\right] \tag{36}$$

where, $\mathbf{P}$ is the vector of parameters to be estimated, $\mathbf{Y}$ is the vector of the experimental measurements, $\hat{\mathbf{Y}}(\mathbf{P})$ is the response of the system applying the estimated parameters, and $\mathbf{W^{-1}}$ is the inverse of the diagonal covariance matrix of

the measurement errors. To minimize the objective function of equation (36), the derivative of the function must be null in relation to each of the unknown parameters. In nonlinear estimation problems, an iterative procedure is necessary, which is obtained by linearizing the vector of the estimated measures, $\hat{\mathbf{Y}}(\mathbf{P})$, with a development in Taylor series around the current solution from *P*. The recurrence equation used in each iteration *k* to mitigate the problem is represented by Eq. (37).

$$\mathbf{P}^{k+1} = \mathbf{P}^{k} + [\,\mathbf{J}^{T}\,\mathbf{W}^{-1}\,\mathbf{J} + \lambda\;\boldsymbol{\Omega}\,]^{-1}\,\mathbf{J}^{T}\,\mathbf{W}^{-1}\,[\mathbf{Y} - \hat{\mathbf{Y}}(\mathbf{P}^{k})] \tag{37}$$

where J represents the Jacobian sensitivity matrix, λ is a positive scalar called the damping parameter and Ω is the matrix with the diagonal terms of $[\mathbf{J}^{\mathrm{T}}\,\mathbf{W}^{-1}\,\mathbf{J}]$. Both, λ and Ω are responsible for damp the fluctuations and the instabilities of the system.

3.2 Sensitivity Analysis

A regular procedure to be performed before the inverse analysis is the sensitivity analysis where the influence of parameters on the systems response is verified. This method allows reducing the dimensionality of the search space. The sensitivity analysis of the suspension coefficients is shown in Figure 4.

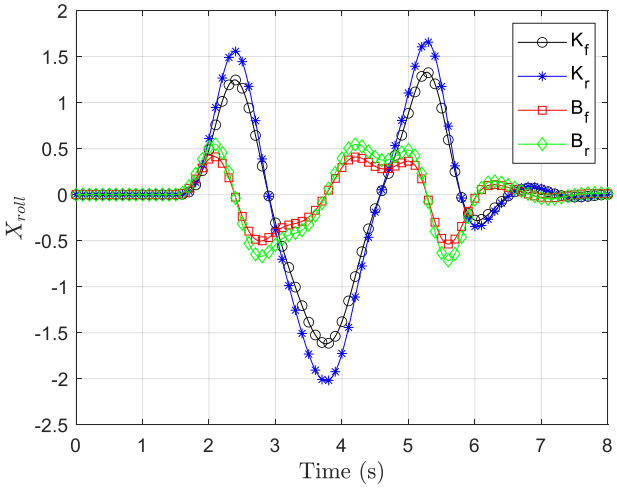

Figure 4. Sensitivity analysis as a function of the roll angle.

The reduced sensitivity coefficient X_{roll}, calculated by taking the first derivative of the roll angle with respect to the suspension constants multiplied by itself. It can be observed that the stiffness coefficients have higher sensitivity coefficients compare to the damping coefficients. Also, the front and rear damping coefficients have strong linear dependence being difficulty to estimate both values at the same time. Due to this analysis, the damping coefficients will be assumed to have a linear behavior, and then they will be estimate as an equivalent damping coefficient.

4. RESULTS ANS DISCUSSIONS

The suspension constants for the 4 DOF vehicle's model, with different loading states (unloaded/loaded) was estimated using inverse problems, by means of the LM method. In order to obtain representative estimations, it is important to avoid convergence to a local minimum value, which could be far from the real value, so it is recommended to perform several estimations to verify if the converged value is the same. The numerical model presented in this work was run in the MATLAB/Simulink® environment considering the simulation of a given vehicle with different load states (unloaded/loaded-Gross vehicle weight (GVW)), as shown in Table 1.

Table 1. Vehicle data with different load states.

Description	Symbol	Unloaded	Loaded
Distance between CG and front axle	a	1.251 m	1.816 m
Distance between CG and rear axle	b	1.834 m	1.269 m
Front/rear gauge	t_f/t_r	1.54 m	1.54 m
Total mass	m_t	2,378 kg	3,378 kg
Sprung mass	m_s	2,124 kg	3,124 kg
Front unsprung mass	m_{uf}	130 kg	130 kg
Rear unsprung mass	m_{ur}	124 kg	124 kg
Height between CG and roll center	h_s	0.46 m	0.61 m
Height of front sprung mass	h_f	0.30 m	0.30 m
Height of rear sprung mass	h_r	0.40 m	0.40 m
Height of CG	h_{cg}	0.80 m	0.95 m
Track adhesion reduction factor	ϵ_r	0.015	0.015
Longitudinal speed	V	11.11 m/s	10 m/s

4.1 Unloaded vehicle

The roll angle response from CarSim® was used as experimental measurements for the LM algorithm. The estimation of the stiffness constants of the front and rear springs, Figure 5a, and the equivalent damping constant, Figure 5b, manage to converge after 12 iterations. The estimations are presented in Table 3.

Table 3. Suspension constants estimations (unloaded vehicle)

Parameter	Symbol	Initial value	Estimated value
Front axle stiffness [N/m]	K_f	40,000	24,3804
Rear axle stiffness [N/m]	K_r	50,000	34,374
Equivalent damping [N s/m]	B_{eq}	16,000	7,502

It is important to highlight in the Figure 5 that the algorithm was adjusting the values of the parameters at each iteration, so that the output of the direct problem using the estimated values is within the established tolerance.

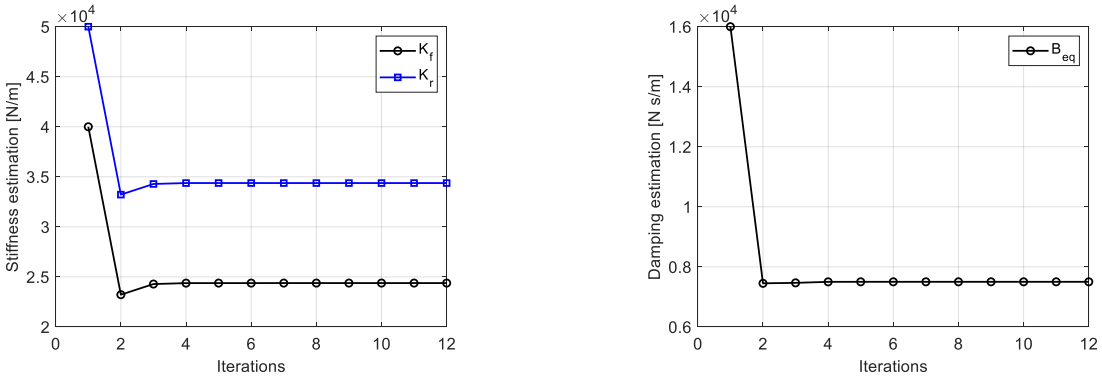

a) Front and rear stiffness estimation. b) Equivalent damping constant estimation

Figure 5. Estimated suspension constants for unloaded vehicle.

In Figure 6, it is possible to observe the dynamic behaviour of the roll angle, where the estimated black curve is compared against the red curve from CarSim® software response. Regarding the estimated curve, it presents a slight divergence to the peak value, with the absolute error of 0.8º, which can be attributed to the simplification of the model compared to CarSim® model (Smith, 2007).

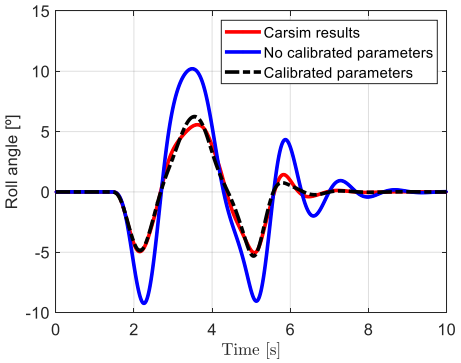

a) Comparative between CarSim data and numerical estimation of the roll angle response

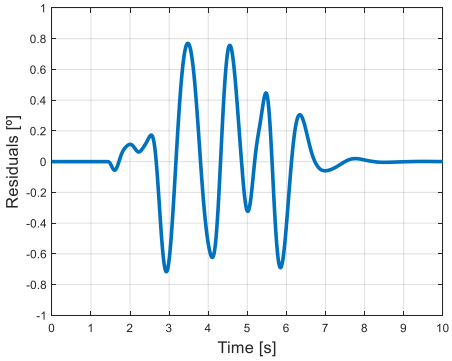

b) Residuals for the roll angle comparative response

Figure 6. Roll angle estimation results.

4.2 Loaded vehicle

Once the unloaded model has been validated, the configuration was changed to the loaded condition presented in Table 1, and the suspension constants was estimated in a double lane change test. In this loaded configuration, the weight was increased with a 1,000 kgf box of 1 m^3. The moments of inertia were recalculated by Steiner's Theorem. The convergence of the parameters was achieved after 18 iterations with the results shown in Table 4.

Table 4. Estimates of suspension constants (loaded vehicle)

Parameter	Symbol	Initial value	Estimated value
Front axle stiffness [*N/m*]	K_f	40,000	28,255
Rear axle stiffness [*N/m*]	K_r	50,000	37,339
Equivalent damping [*N s/m*]	B_{eq}	16,000	7,254

The convergence evolution of estimated parameters is presented in Figure 7. The converged values were used as input to the direct problem and the comparison of the numerical response with CarSim® measurements are presented in Figure 8. Figure 8 also shows the improvement of the curve due to the estimation process, which indicates that the initial parameters are incorrect. In all the analyses, the convergence of the suspension parameters is performed by the LM Method, where the applied estimation allowed to satisfactorily improve the roll angle of the sprung mass during the double lane change test compared to the results with no calibrated parameters.

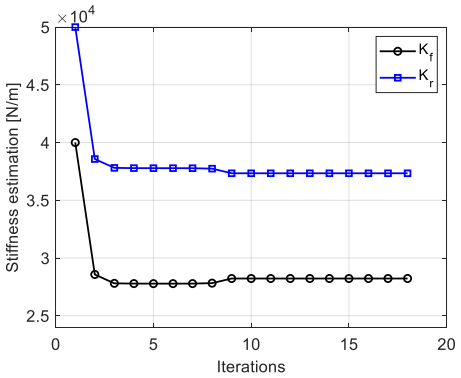

a) Front and rear stiffness estimation.

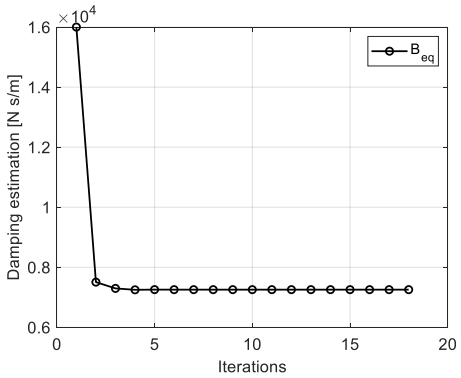

b) Equivalent damping constants estimation.

Figure 7. Estimated suspension constants for loaded vehicle.

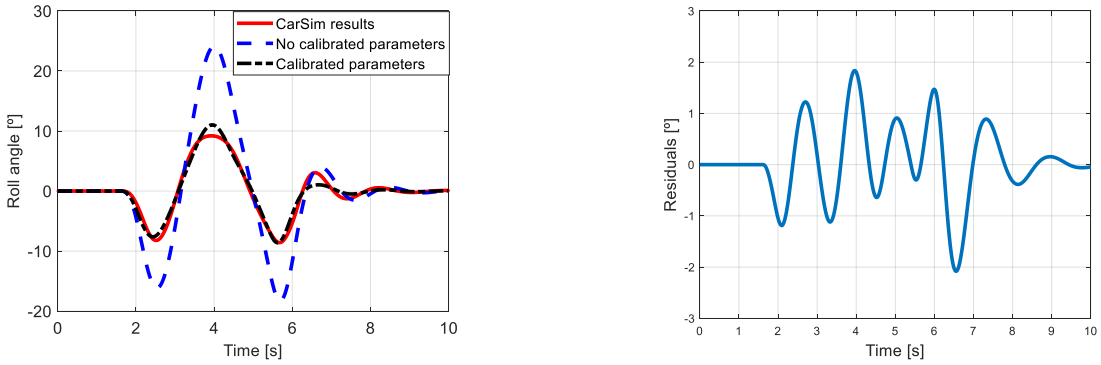

a) Comparative between CarSim data and numerical estimation of the roll angle response

b) Residuals for the roll angle comparative response

Figure 8. Roll angle with estimated suspension parameters for loaded vehicle.

5. CONCLUSIONS

This work allows a better understanding of the suspension role of a pickup truck during a curve maneuver, using a non-linear 4 DOF model. The approach of the power flow method (Costa Neto, 2001) allowed an integration of the subsystems and systems, making easier the interpretation of the behavior according to the connection order. By using a non-linear tire model (Dugoff, 1970), it was possible to simulate the combined forces generated in the contact area of the tire, allowing the double lane change test to be carried out in acceptable terms. The sensitivity analysis allowed the focus on the most representative parameters in the estimation process, using the Levenberg-Marquardt method, providing the estimation of vital parameters for the development and solution of mathematical models, reducing data uncertainties. The use of a vehicle development tool as CarSim allowed to verify the computational simulation of the model without the need to perform an experimental test, providing consistent dynamic responses, also helping to reduce time, accident risks and development costs in initial stages of the project. Despite the small and eventual discrepancies found, the simulations conducted in the present work proved to be effective in the analysis of critical operational situations, allowing the improvement of the conceptual design of a vehicle.

6. REFERENCES

Campos, C. Estimativa dos coeficientes de rigidez e amortecimento para um veículo leve. Revista Militar de Ciência e Tecnologia, v. 367, 2017. Disponível em: < http://rmct.ime.eb.br/arquivos/ RMCT_2_sem_2017/RMCT_367 MEC_2017.pdf>.

CarSim, 2020. “Carsim-Mechanical Simulation-Virtual CAE”. https://www.carsim.com/products/carsim/. Mechanical Simulation Corporation.

Cortez, O., 2004. Aplicação do método de Levenberg-Marquardt/Gradiente conjugado na estimativa de calor de um aparelho de placa quente com proteção. Master’s thesis, Centro Nacional de Pesquisa e Desenvolvimento Tecnológico Cuernavaca, Morelos, México.

Costa Neto, R.T., 2001. Modelo de veículo Tipo 4 WS utilizando transformadores cinemáticos. Master’s thesis, Instituto Militar de Engenharia, Rio de Janeiro.

Dugoff, H., 1970. “An analysis of tire properties and their influence on vehicle dynamic performance”. SAE, Vol. 79. Section 2, paper number 700377, page 1219-1243.

Gillespie, T., 1992. Fundamental of Vehicle Dynamics. Society of Automotive Engineers, Inc, (SAE), Pensilvania, USA.

Jazar, R., 2008. Vehicle Dynamics. Springer, New York, USA.

Leão Pereira, C. Implementação computacional e análise do emprego de um sistema de controle de assistência ao motorista em um modelo de veículo 6x6. 106 p. Mestrado em Engenharia — Instituto Militar de Engenharia, Rio de Janeiro, 2020. Disponível em: <http://www.ime.eb.mil.br/images/arquivos/pos-graduacao/mecanica/2020_ Dissertacao_Camila_Leao_Pereira.pdf>.

Leão Pereira, C., Costa Neto, R.T., and Loiola, B.R., 2021. “Cornering stiffness estimation using Levenberg–Marquardt approach”. *Inverse Problems in Science and Engineering*, pp. 1–32. https://doi.org/10.1080/17415977.2021.1910683.

Lima spinola, A., 2003. *Modeling and non linear control of a ground vehicle’s steering* (in Portuguese). Master’s thesis, Graduate Program in Electrical Engineering, Pontifícia Universidade Católica-PUC Rio, Rio de Janeiro, Brazil.

Smith, 2007. “Effects of model complexity on the performance of automated vehicle steering controllers: Model development, validation and comparison”. Vehicle System Dynamics, Vol. 24. Pp 161-181.

Will, A. and AK, S.H.Z., 1997. “Modelling and control of an automated vehicle”. Vehicle System Dynamics, Vol. 27, pp. 131–155.

7. RESPONSIBILITY NOTICE

The authors are the only responsible for the printed material included in this paper.